

Chapter 10

Dyson Equation and Self-Consistent Green's functions

The results of Ch. 9 represent an important link between the sp propagator of a correlated system and the two known ingredients represented by the two-body interaction \hat{V} and the noninteracting ground state $|\Phi_0^A\rangle$. The latter state may require the introduction of an auxiliary one-body potential \hat{U} . One may assume the relevant one-body problem of $H_0 = T + U$ to be solvable. The corresponding lowest levels of this Hamiltonian may therefore be filled in accordance with the total number of particles and the Pauli principle to obtain the corresponding noninteracting ground state represented by $|\Phi_0^A\rangle$ as discussed in Chs. 3 and 5. Having established the complete perturbation expansion of the exact propagator G in Ch. 9 in terms of these known quantities, by no means suggests a proper way to select contributions to be included for a meaningful description of the system under study.

It is the purpose of this chapter to develop a systematic approach based on perturbation theory to describe physically interesting many-particle systems. All systems of interest require a treatment that goes beyond the usual perturbation theory developed for one-body systems [Messiah (1999)]. Indeed, it may be useful to note that adding the first-order contribution, $G_V^{(1)}$ given by Eq. (9.61) and shown in Fig. 9.16, to the noninteracting propagator $G^{(0)}$ does not represent a useful approximation to the problem even if the two-body interaction \hat{V} would be small in some way. The reason for this inadequacy is the observation that the resulting approximation does not have important properties that one assigns to the exact propagator. For example, the sum of $G^{(0)}$ and $G_V^{(1)}$ does not have a Lehmann representation and can therefore not be interpreted as containing information describing the removal and addition probabilities of particles with respect to the ground state of the system. Also the energies of the states of the

system with one or more particle cannot be extracted from this approximation. These observations become immediately clear when one realizes that the diagonal elements of $G^{(1)}$ have a double pole at the sp energy corresponding to the one of $G^{(0)}$ whereas the exact sp propagator has simple poles (at different energies). To obtain approximations that share such features it is necessary to reorganize the perturbation expansion in such a way that it automatically leads to the summation of infinite sets of diagrams. The relevant analysis is described in Sec. 10.1 and leads to the so-called Dyson equation and the introduction of the self-energy of a particle in the medium.

At this stage, one has a tool in hand to generate interesting descriptions of the sp propagator by making approximations to the self-energy. There is, however, one more ingredient missing in this strategy. This ingredient is related to the notion that the evaluation of the self-energy even as presented in Ch. 9 involves the use of noninteracting propagators. Physically it makes more sense to let the particle considered explicitly in the Dyson equation, interact with particles in the medium which, in turn, also experience the same correlations as one is trying to include for the particle under study. This democratic notion leads to the important concept of self-consistency between the solution of the Dyson equation and the ingredients which make up the corresponding self-energy. This concept is best developed formally by studying the equations of motion for the sp propagator as presented in Sec. 10.3. This study reveals a dynamic coupling between the sp propagator and the two-particle propagator in the medium which is the subject of study in Sec. 10.4. This two-particle propagator can be studied by analyzing its perturbation expansion in exactly the same way as was done for the sp propagator. This analysis leads to the introduction of the vertex function which can be interpreted as the effective interaction between particles which are fully correlated in the medium and therefore themselves described in terms of exact sp propagators. All these results are then combined at the end of Sec. 10.4 to obtain the self-energy of a particle in terms of this vertex function.

The Dyson equation can be regarded as the Schrödinger equation of a particle in the medium subject to the self-energy as the potential. This interpretation is further developed in Sec. 10.5 and its relation with the analysis of experimental data from particle knockout experiments is emphasized (see also Ch. 8). At this point, the stage is set to study many-particle systems of interest since all relevant ingredients like the Dyson equation and self-consistency are now available. It is then possible to choose approx-

imation schemes based on information concerning the two-body propagator in the medium. This information is provided by considering relevant experimental data sometimes in the form of two-particle scattering results. The simplest case, involving a rather weak interaction, generates the Hartree-Fock scheme to be discussed in detail in Ch. 11. Its extension to include the next higher-order contribution is discussed in Ch. 13. Systems with stronger correlations require other approximation schemes involving infinite summations as relevant approximations to the effective two-body interaction in the medium. These approximations and their applications will be discussed in subsequent chapters.

10.1 Analysis of perturbation expansion, self-energy, and Dyson's equation

In the last section of Ch. 9, the energy formulation of the diagrammatic expansion of the propagator was introduced. From the discussion in the last part of Sec. 9.5.2 one can infer that it is possible to obtain a diagrammatic representation of the propagator as shown in Fig. 10.1. In this figure the convention is introduced that the exact sp propagator is represented by two arrowed lines. The observation that any term in the perturbation expansion of G except the zero-order one has a noninteracting propagator at the top and at the bottom of the diagram makes it possible to introduce the self-energy Σ which represents the sum of all the contributions between this first and last unperturbed propagator. This decomposition of the sp propagator in the noninteracting propagator $G^{(0)}$ and the sum of the other terms defin-

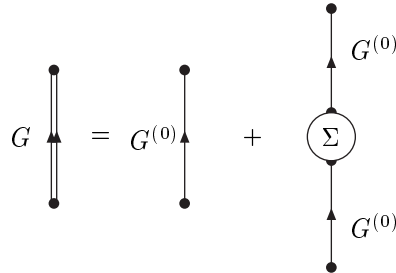
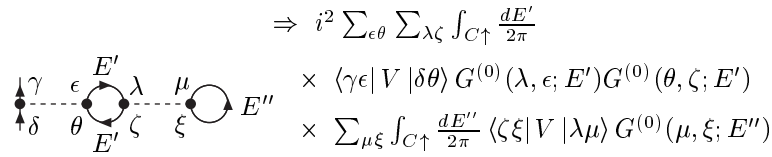


Fig. 10.1 Diagrammatic representation of the sp propagator introducing the reducible self-energy Σ .

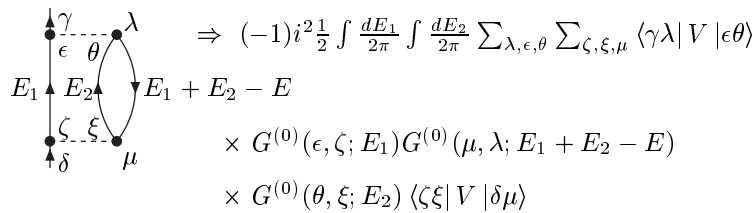


$$\Rightarrow i^2 \sum_{\epsilon\theta} \sum_{\lambda\zeta} \int_{C^+} \frac{dE'}{2\pi} \times \langle \gamma\epsilon | V | \delta\theta \rangle G^{(0)}(\lambda, \epsilon; E') G^{(0)}(\theta, \zeta; E') \times \sum_{\mu\xi} \int_{C^+} \frac{dE''}{2\pi} \langle \zeta\xi | V | \lambda\mu \rangle G^{(0)}(\mu, \xi; E'')$$

Fig. 10.4 Diagram SE2e for the self-energy in second order

sp propagator leading to an unambiguous definition of the self-energy as illustrated in Fig. 10.1. Additional contributions in first and second order occur when the auxiliary sp potential \hat{U} is employed. These additional self-energy diagrams are shown in Fig. 10.6. Based on the rules developed for the diagrams contributing to the sp propagator, it is quite straightforward to generate the expressions for the self-energy terms depicted in Figs. 10.6a) - 10.6e).

It is now possible to divide the self-energy contributions shown in Figs. 10.2 - 10.6 into two categories. The first category contains terms that are called irreducible. The sum of all these contributions to the self-energy including all the higher-order terms, is denoted by Σ^* . The diagrams shown in Figs. 10.2, 10.4, 10.5, 10.6a), and 10.6b) belong to this category. The word irreducible means here that such diagrams do not contain two (or more) parts that are only connected by an unperturbed sp propagator $G^{(0)}$. All other contributions to the self-energy are called reducible. Together with the irreducible ones they comprise all contributions to Σ . Analysis



$$\Rightarrow (-1)i^{2\frac{1}{2}} \int \frac{dE_1}{2\pi} \int \frac{dE_2}{2\pi} \sum_{\lambda, \epsilon, \theta} \sum_{\zeta, \xi, \mu} \langle \gamma\lambda | V | \epsilon\theta \rangle \times G^{(0)}(\epsilon, \zeta; E_1) G^{(0)}(\mu, \lambda; E_1 + E_2 - E) \times G^{(0)}(\theta, \xi; E_2) \langle \zeta\xi | V | \delta\mu \rangle$$

Fig. 10.5 Diagram SE2i for the self-energy in second order

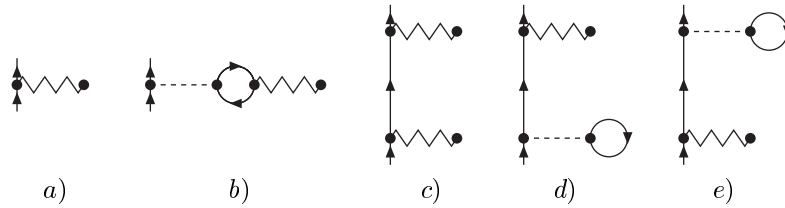


Fig. 10.6 Additional diagrams contributing to the self-energy up to second order when an auxiliary potential U is employed.

of the structure of the diagrams contributing to the sp propagator makes it clear that the irreducible self-energy suffices to obtain the propagator. The corresponding diagrammatic result is shown in Fig. 10.7. This figure illustrates how successive iterations of the irreducible self-energy Σ^* linked by the unperturbed propagator $G^{(0)}$ will generate all terms contributing to the sp propagator. The irreducible self-energy diagrams like Figs. 10.2 etc. contribute to the sp propagator in the term with one insertion of the irreducible self-energy on the right side of Fig. 10.7. The second-order reducible self-energy diagrams like Figs. 10.3 etc. appear in the next term with two irreducible self-energy insertions. Higher-order self-energy contributions distribute themselves over the terms schematically indicated in Fig. 10.7 in a similarly unique fashion.

This analysis indicates that all contributions to the sp propagator can be obtained from the irreducible terms by summing the following expression.

$$\begin{aligned}
 G(\alpha, \beta; E) &= G^{(0)}(\alpha, \beta; E) \\
 &+ \sum_{\gamma, \delta} G^{(0)}(\alpha, \gamma; E) \Sigma^*(\gamma, \delta; E) G^{(0)}(\delta, \beta; E) \\
 &+ \sum_{\gamma, \delta, \epsilon, \theta} G^{(0)}(\alpha, \gamma; E) \Sigma^*(\gamma, \epsilon; E) G^{(0)}(\epsilon, \theta; E) \Sigma^*(\theta, \delta; E) G^{(0)}(\delta, \beta; E) \\
 &+ \dots
 \end{aligned} \tag{10.1}$$

This equation exactly represents the diagrams shown in Fig. 10.7. In Ch. 7 a similar equation was discussed for the sp propagator in the sp problem. Possible resummations of the corresponding Eq. (7.19) for the operator form of G were discussed there. A similar set of resummations will be considered here for Eq. (10.1). There are several equivalent ways to sum the right hand side of Eq. (10.1). To visualize this resummation strategy several lines have been drawn in Fig. 10.7. Considering first the short-dashed lines, they help identify two ways of obtaining the so-called Dyson

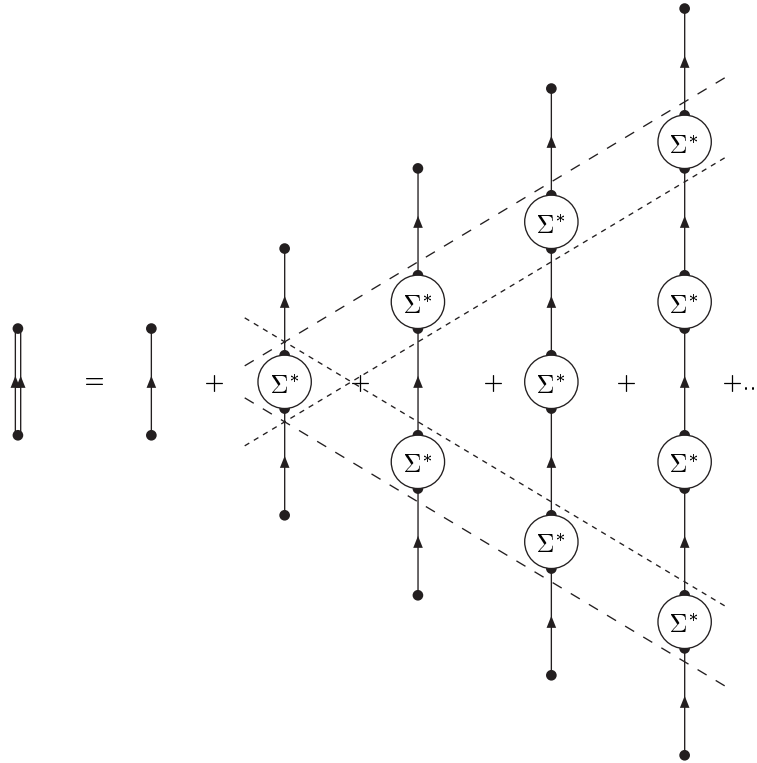


Fig. 10.7 Decomposition of the sp propagator in terms of irreducible self-energy contributions.

equation for the sp propagator. Indeed, by identifying all terms below the short-dashed line with the positive slope as the sum of all contributions to the sp propagator, one may rewrite Eq. (10.1) according to

$$G(\alpha, \beta; E) = G^{(0)}(\alpha, \beta; E) + \sum_{\gamma, \delta} G^{(0)}(\alpha, \gamma; E) \Sigma^*(\gamma, \delta; E) G(\delta, \beta; E). \quad (10.2)$$

Alternatively, one also identifies all contributions above the short-dashed line with the negative slope in Fig. 10.7 with the full sp propagator so that one may also write

$$G(\alpha, \beta; E) = G^{(0)}(\alpha, \beta; E) + \sum_{\gamma, \delta} G(\alpha, \gamma; E) \Sigma^*(\gamma, \delta; E) G^{(0)}(\delta, \beta; E). \quad (10.3)$$

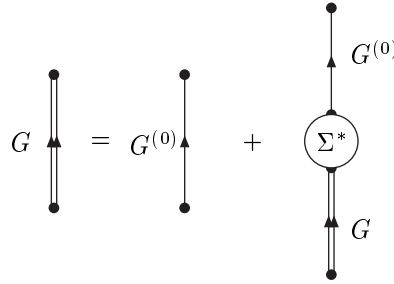


Fig. 10.8 Diagrammatic representation of the sp propagator in terms of the irreducible self-energy Σ^* and the noninteracting propagator $G^{(0)}$ representing Eq. (10.2).

Equation (10.2) is shown diagrammatically in Fig. 10.8. A similar diagrammatic representation can be obtained for Eq. (10.3) by interchanging $G^{(0)}$ and G in the second term on the right side in Fig. 10.8. As in the case of the sp problem, the infinite summation form of Eqs. (10.2) and (10.3) makes it possible to construct eigenvalue problems in the case of discrete solutions for the energy to these equations. The nonperturbative aspect of this form of the Dyson equation makes it possible to obtain approximate solutions to the sp propagator which can be interpreted in the same way as the exact propagator. This includes the presence of simple poles at the approximate energies of states with one particle more or less than the ground state (with respect to the approximate energy of the ground state). The numerator of this approximate propagator then contains corresponding approximate addition and removal amplitudes as the exact propagator (see the discussion in Ch. 8).

Comparing the reducible self-energy shown in Fig. 10.1 with the expansion shown in Fig. 10.7, it is clear that the reducible self-energy is the sum of all terms inside the boundaries of the two long-dashed lines in that figure (a similar result was obtained in Ch. 7 for the T -matrix in the sp case). This identification leads to the following the following result

$$\begin{aligned}
 \Sigma(\gamma, \delta; E) &= \Sigma^*(\gamma, \delta; E) \\
 &+ \sum_{\epsilon, \theta} \Sigma^*(\gamma, \epsilon; E) G^{(0)}(\epsilon, \theta; E) \Sigma^*(\theta, \delta; E) \\
 &+ \sum_{\epsilon, \theta, \zeta, \xi} \Sigma^*(\gamma, \epsilon; E) G^{(0)}(\epsilon, \theta; E) \Sigma^*(\theta, \zeta; E) G^{(0)}(\zeta, \xi; E) G^{(0)}(\xi, \delta; E) \\
 &+ \dots
 \end{aligned} \tag{10.4}$$

This result can also be summed in two ways reminiscent of the Dyson equation with its two equivalent forms given by Eqs. (10.2) and (10.3). One can again make use of the symmetry of Fig. 10.7 to obtain

$$\Sigma(\gamma, \delta; E) = \Sigma^*(\gamma, \delta; E) + \sum_{\epsilon, \theta} \Sigma^*(\gamma, \epsilon; E) G^{(0)}(\epsilon, \theta; E) \Sigma(\theta, \delta; E) \quad (10.5)$$

or

$$\Sigma(\gamma, \delta; E) = \Sigma^*(\gamma, \delta; E) + \sum_{\epsilon, \theta} \Sigma(\gamma, \epsilon; E) G^{(0)}(\epsilon, \theta; E) \Sigma^*(\theta, \delta; E). \quad (10.6)$$

These equations are the equivalent of the Lippmann-Schwinger equation for the T -matrix in the case of a sp problem (see Eqs. (7.20) and (7.21) and can therefore be used in the case of problems involving a continuous spectrum. The irreducible self-energy Σ^* therefore plays a role very similar to the potential in the sp problem. Note, however, that in the many-particle problem the influence of the medium leads to an energy-dependent complex potential represented by the irreducible self-energy.

10.2 Equation of motion method for propagators

The present analysis of the diagrammatic expansion introduces the concept of the self-energy without yielding a clear strategy on how to decide which approximations will have to be made in order to describe realistically the correlations in the system under study. The importance of the Dyson equation is related to the infinite summation it represents. Infinite summations allow for results that are not possible to obtain using order by order summation of perturbation contributions. An example is provided by the possibility of generating bound states from a noninteracting propagator corresponding to a continuum spectrum.

An algebraic method for deriving the Dyson equation also exists [Abrikosov *et al.* (1975)]. This method gives a better insight into the possible strategies available for dealing with the most important correlations in the system and, subsequently, taking those correlations into account in the self-energy. This approach starts with the equation of motion for the sp propagator. This requires a return to the time formulation. In order to study the time derivative of the sp propagator it is useful to consider the corresponding derivatives of the addition and removal operator

in the Heisenberg picture as given by Eq. (A.38) leading to

$$i\hbar \frac{\partial}{\partial t} a_{\alpha_H}(t) = [a_{\alpha_H}(t), \hat{H}] = \exp\{i\hat{H}t/\hbar\} [a_{\alpha}, \hat{H}] \exp\{-i\hat{H}t/\hbar\}. \quad (10.7)$$

for the removal operator for example. The Hamiltonian \hat{H} will include the auxiliary potential in \hat{H}_0 and will therefore be decomposed according to

$$\hat{H} = \hat{H}_0 - \hat{U} + \hat{V}. \quad (10.8)$$

Using the sp basis that diagonalizes H_0 one has

$$\hat{H}_0 = \sum_{\gamma} \varepsilon_{\gamma} a_{\gamma}^{\dagger} a_{\gamma}. \quad (10.9)$$

The three commutators required for Eq. (10.7) then yield

$$[a_{\alpha}, \hat{H}_0] = \varepsilon_{\alpha} a_{\alpha}, \quad (10.10)$$

$$[a_{\alpha}, \hat{U}] = \sum_{\delta} \langle \alpha | U | \delta \rangle a_{\delta} \quad (10.11)$$

using the conjugate of Eq. (2.34), and

$$[a_{\alpha}, \hat{V}] = \frac{1}{2} \sum_{\delta\zeta\theta} \langle \alpha\delta | V | \theta\zeta \rangle a_{\delta}^{\dagger} a_{\zeta} a_{\theta} \quad (10.12)$$

using the conjugate of Eq. (2.42) for the symmetrized version of \hat{V} given in Eq. (2.46). Inserting the results of Eqs. (10.10) - (10.12) into Eq. (10.7) yields

$$\begin{aligned} i\hbar \frac{\partial}{\partial t} a_{\alpha_H}(t) &= \varepsilon_{\alpha} a_{\alpha_H}(t) - \sum_{\delta} \langle \alpha | U | \delta \rangle a_{\delta_H}(t) \\ &+ \frac{1}{2} \sum_{\delta\zeta\theta} \langle \alpha\delta | V | \theta\zeta \rangle a_{\delta_H}^{\dagger}(t) a_{\zeta_H}(t) a_{\theta_H}(t). \end{aligned} \quad (10.13)$$

It is now possible with the help of Eq. (10.13) to establish the time derivative of the sp propagator but first one uses the step function decomposition of the time-ordering operation to obtain

$$\begin{aligned} i\hbar \frac{\partial}{\partial t} G(\alpha, \beta; t - t') &= \frac{\partial}{\partial t} \langle \Psi_0^A | \mathcal{T}[a_{\alpha_H}(t) a_{\beta_H}^{\dagger}(t')] | \Psi_0^A \rangle \\ &= \langle \Psi_0^A | \frac{\partial}{\partial t} \left\{ \theta(t - t') a_{\alpha_H}(t) a_{\beta_H}^{\dagger}(t') - \theta(t' - t) a_{\beta_H}^{\dagger}(t') a_{\alpha_H}(t) \right\} | \Psi_0^A \rangle. \end{aligned} \quad (10.14)$$

Evaluating all the time derivatives contributing to Eq. (10.14), and substituting Eq. (10.13) one obtains

$$\begin{aligned}
 i\hbar \frac{\partial}{\partial t} G(\alpha, \beta; t - t') &= \delta(t - t') \delta_{\alpha\beta} + \langle \Psi_0^A | \mathcal{T} \left[\frac{\partial a_{\alpha_H}(t)}{\partial t} a_{\beta_H}^\dagger(t') \right] | \Psi_0^A \rangle \quad (10.15) \\
 &= \delta(t - t') \delta_{\alpha\beta} + \varepsilon_\alpha G(\alpha, \beta; t - t') - \sum_{\delta} \langle \alpha | U | \delta \rangle G(\delta, \beta; t - t') \\
 &\quad + \frac{-i}{2\hbar} \sum_{\delta\zeta\theta} \langle \alpha\delta | V | \theta\zeta \rangle \langle \Psi_0^A | \mathcal{T} [a_{\delta_H}^\dagger(t) a_{\zeta_H}(t) a_{\theta_H}(t) a_{\beta_H}^\dagger(t')] | \Psi_0^A \rangle.
 \end{aligned}$$

Eq.(10.15) represents the first step of a hierarchy in which the $A+1$ -particle propagator is related to the A -particle propagator [Martin and Schwinger (1959); Migdal (1967)]. In the present example, this coupling is established between the sp and the two-particle propagator which is contained in the last line of Eq. (10.15). This two-particle propagator is in turn related to the three-particle propagator, etc. Before continuing the construction of the irreducible self-energy, it is first necessary to analyze the diagrammatic content of the two-particle propagator. This is accomplished in the next section.

10.3 Two-particle propagator, vertex function, and self-energy

The two-particle (tp) propagator is defined in analogy with the sp propagator (Eq. (8.1)) and given by

$$G_{II}(\alpha t_\alpha, \beta t_\beta, \gamma t_\gamma, \delta t_\delta) = -\frac{i}{\hbar} \langle \Psi_0^A | \mathcal{T} [a_{\beta_H}(t_\beta) a_{\alpha_H}(t_\alpha) a_{\gamma_H}^\dagger(t_\gamma) a_{\delta_H}^\dagger(t_\delta)] | \Psi_0^A \rangle. \quad (10.16)$$

The steps taken for the sp propagator leading to Eq. (9.54) may now be repeated for the two-particle (tp) propagator. In the attaining this expression for the two-particle propagator the Heisenberg picture addition and removal operators have then been replaced by corresponding interaction picture operators and the expectation value is taken with respect to the noninteracting ground state $|\Phi_0^A\rangle$. Application of Wick's theorem to the equivalent result of Eq. (9.17) for every term in the resulting perturbation expansion again reveals a cancellation between the numerator and the denominator leading to a corresponding set of connected contributions

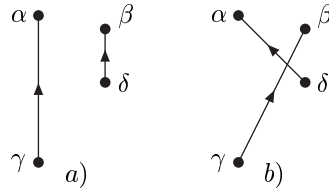


Fig. 10.9 The two contributions to the noninteracting tp propagator in the time formulation as given by Eq. (10.18).

(diagrams). This result may be written as

$$G_{II}(\alpha t_\alpha, \beta t_\beta, \gamma t_\gamma, \delta t_\delta) = -\frac{i}{\hbar} \sum_m \left(\frac{-i}{\hbar}\right)^m \frac{1}{m!} \int dt_1 \dots \int dt_m \quad (10.17)$$

$$\times \langle \Phi_0^A | \mathcal{T} [\hat{H}_1(t_1) \dots \hat{H}_1(t_m) a_\beta(t_\beta) a_\alpha(t_\alpha) a_\gamma^\dagger(t_\gamma) a_\delta^\dagger(t_\delta)] | \Phi_0^A \rangle_{connected}.$$

and is indeed the equivalent of Eq. (9.54) and the details of the intermediate steps require only minor changes which will be left to the reader. The notion of connected diagrams in the context of Eq. (10.17) requires a little clarification that will be given below.

In zero order, one obtains the noninteracting tp propagator

$$G_{II}^{(0)}(\alpha t_\alpha, \beta t_\beta, \gamma t_\gamma, \delta t_\delta) = -\frac{i}{\hbar} \langle \Phi_0^A | \mathcal{T} [a_\beta(t_\beta) a_\alpha(t_\alpha) a_\gamma^\dagger(t_\gamma) a_\delta^\dagger(t_\delta)] | \Phi_0^A \rangle$$

$$= i\hbar [G^{(0)}(\alpha, \gamma; t_\alpha - t_\gamma) G^{(0)}(\beta, \delta; t_\beta - t_\delta)$$

$$- G^{(0)}(\alpha, \delta; t_\alpha - t_\delta) G^{(0)}(\beta, \gamma; t_\beta - t_\gamma)]. \quad (10.18)$$

This combination of unperturbed sp propagators is shown diagrammatically in Fig. 10.9. Also here, no time-ordering is assumed since we are dealing again with Feynman diagrams. Clearly, “disconnected” should not apply to the two noninteracting propagators shown in Fig. 10.9. Similarly, higher-order contributions which have attachments to these lines but do not connect the two lines are still connected as long as there are no other parts to the diagram which do not link to these two lines.

For the analysis of the two-particle propagator in higher order it is useful to rewrite the \hat{V} contribution in \hat{H}_1 in a more general way. This will allow a generalization of \hat{V} that will include these higher-order corrections. By including additional time integrals one can rewrite the interaction picture

\hat{V} as follows

$$\begin{aligned}\hat{V}(t_1) &= \int dt_1 \frac{1}{4} \sum_{\alpha\beta\gamma\delta} \langle \alpha\beta | V | \gamma\delta \rangle a_\alpha^\dagger(t_1) a_\beta^\dagger(t_1) a_\delta(t_1) a_\gamma(t_1) \\ &= \int dt_1 \int dt_2 \int dt_3 \int dt_4 \frac{1}{4} \sum_{\alpha\beta\gamma\delta} \langle \alpha\beta | V(t_1, t_2; t_3, t_4) | \gamma\delta \rangle \\ &\quad \times a_\alpha^\dagger(t_1) a_\beta^\dagger(t_2) a_\delta(t_4) a_\gamma(t_3),\end{aligned}\quad (10.19)$$

where

$$\langle \alpha\beta | V(t_1, t_2; t_3, t_4) | \gamma\delta \rangle = \delta(t_1 - t_2) \delta(t_2 - t_3) \delta(t_3 - t_4) \langle \alpha\beta | V | \gamma\delta \rangle. \quad (10.20)$$

With this generalization in place, one may proceed by analyzing the first and higher order contributions to Eq. (10.17).

Using the formulation of \hat{V} given in Eq. (10.19), the corresponding first-order contribution generates the following result

$$\begin{aligned}G_{II}^{(1)}(\alpha t_\alpha, \beta t_\beta, \gamma t_\gamma, \delta t_\delta) &\Rightarrow \\ &\left(\frac{-i}{\hbar}\right)^2 \int dt_1 \int dt_2 \int dt_3 \int dt_4 \frac{1}{4} \sum_{abcd} \langle ab | V(t_1, t_2; t_3, t_4) | cd \rangle \\ &\langle \Phi_0^A | \mathcal{T} \left[a_\alpha^\dagger(t_1) a_\beta^\dagger(t_2) a_\delta(t_4) a_\gamma(t_3) a_\beta(t_\beta) a_\alpha(t_\alpha) a_\gamma^\dagger(t_\gamma) a_\delta^\dagger(t_\delta) \right] | \Phi_0^A \rangle \\ &= (i\hbar)^2 \int dt_1 \int dt_2 \int dt_3 \int dt_4 \sum_{abcd} \langle ab | V(t_1, t_2; t_3, t_4) | cd \rangle \\ &\quad \times G^{(0)}(\alpha, a; t_\alpha - t_1) G^{(0)}(\beta, b; t_\beta - t_2) \\ &\quad \times G^{(0)}(c, \gamma; t_3 - t_\gamma) G^{(0)}(d, \delta; t_d - t_\delta).\end{aligned}\quad (10.21)$$

In establishing this result Wick's theorem and the symmetry of \hat{V} was used while only the connected contributions were kept. In addition, those contributions that link the interaction to only one of the sp propagators (corresponding to self-energy insertion) have also been suppressed. Diagrammatically, one may replace the dashed line for \hat{V} by a box to represent the additional time arguments to anticipate the subsequent discussion of higher-order terms. Such a diagrammatic representation of Eq. (10.21) is given in Fig. 10.10.

In the analysis of the sp propagator two types of diagrams were encountered. The first kind only contained the diagram representing $G^{(0)}$. The second kind contained all other connected diagrams involving higher-order self-energy insertions as illustrated in Fig. 10.1. The tp propagator also

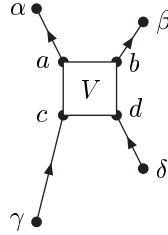


Fig. 10.10 First-order connected contribution to the tp propagator linking two noninteracting propagators in the time formulation.

contains two types of diagrammatic contributions. The first group includes the diagram with two noninteracting sp propagators shown in Fig. 10.9. In higher order, additional terms are generated which contribute to this same group. These terms are just those contributions which insert all possible self-energy corrections to these noninteracting propagators but never link the two. As a result, one identifies in higher order all the contributions which generalize the diagrams in Fig. 10.9 to fully correlated and exact sp propagators. This extension of Fig. 10.9 is shown in part *a*) of Fig. 10.11. Note that the dressing will include both the generalization of part *a*) and *b*) of Fig. 10.9.

The other group of diagrams which are obtained in higher order are generalizations of the connected first-order contribution. Also in this case all four noninteracting propagators shown in Fig. 10.10 will receive all possible

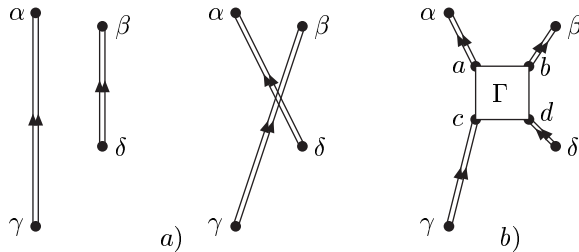


Fig. 10.11 Two contributions to the exact tp propagator in the time formulation. In part *a*) the dressed but noninteracting tp propagator is shown including both direct and exchange contribution. In part *b*) the four-point vertex function Γ is introduced to represent the sum of all higher-order contributions generalizing Fig. 10.10.

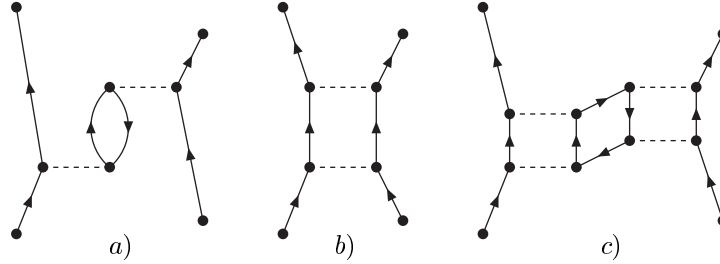


Fig. 10.12 Higher-order connected contributions to the tp propagator which generalize the first-order term in Fig. 10.10 to the four-point vertex function.

self-energy insertions turning all four propagators into exact sp propagators. This, however, is not the only extension of Fig. 10.10 that is possible. In addition to dressing the propagators, more complicated connections appear which connect the incoming two propagators with the two outgoing ones. Examples of such generalizations are shown in Fig. 10.12. In this figure the usual dash-line for the interaction V has been used to emphasize the actual time structure of these diagrams. Also, no additional insertions were included in the four external sp propagators. In the diagrams shown in Figs. 10.12a) and 10.12b) the interaction between the two incoming and two outgoing sp propagators is characterized by two times, whereas the corresponding interaction in Fig. 10.12c) has four different times. The latter term is an example illustrating the necessity to generalize V to a four-point vertex function Γ when higher-order contributions are taken into account. This four-point vertex function includes all possible terms that connect the two incoming lines with the two outgoing ones. All intermediate sp propagators will correspondingly become fully dressed as well as the four external ones in the diagrams shown in Fig. 10.12. This also holds for all other higher-order contributions.

By replacing the unperturbed sp propagators by dressed ones and replacing V by the sum of all diagrams that connect these particle lines represented by the box labeled Γ in Fig. 10.11, one obtains in this way the other group of contributions to G_{II} [Abrikosov *et al.* (1975)]. Γ is referred to as the four-point vertex function since it has four external points. This quantity can be considered as the effective interaction between dressed particles in the medium. It is now possible to summarize this discussion by

writing G_{II} in terms of dressed sp proapgators and Γ as follows

$$\begin{aligned}
G_{II}(\alpha t_\alpha, \beta t_\beta, \gamma t_\gamma, \delta t_\delta) = & \\
& i\hbar[G(\alpha, \gamma; t_\alpha - t_\gamma)G(\beta, \delta; t_\beta - t_\delta) - G(\alpha, \delta; t_\alpha - t_\delta)G(\beta, \gamma; t_\beta - t_\gamma)] \\
& + (i\hbar)^2 \int dt_a \int dt_b \int dt_c \int dt_d \sum_{a,b,c,d} G(\alpha, a; t_\alpha - t_a)G(\beta, b; t_\beta - t_b) \\
& \times \langle ab | \Gamma(t_a, t_b, t_c, t_d) | cd \rangle G(c, \gamma; t_c - t_\gamma)G(d, \delta; t_d - t_\delta). \quad (10.22)
\end{aligned}$$

This is the result shown diagrammatically in Fig. 10.11.

10.4 Dyson equation and the vertex function

It is now possible to return to Eq. (10.15) to complete the analysis of the equation of motion for the propagator G . The general result for the tp propagator obtained in Eq. (10.22) can now be inserted into Eq. (10.15)

$$\begin{aligned}
i\hbar \frac{\partial}{\partial t} G(\alpha, \beta; t - t') = & \delta(t - t')\delta_{\alpha\beta} + \varepsilon_\alpha G(\alpha, \beta; t - t') \\
& - \sum_\delta \langle \alpha | U | \delta \rangle G(\delta, \beta; t - t') \\
& - i\hbar \sum_{\delta\zeta\theta} \langle \alpha\delta | V | \theta\zeta \rangle G(\zeta, \delta; t - t^+)G(\theta, \beta; t - t') \\
& - \frac{1}{2}(i\hbar)^2 \sum_{\delta\zeta\theta} \sum_{abcd} \int dt_a \int dt_b \int dt_c \int dt_d \langle \alpha\delta | V | \theta\zeta \rangle \\
& \times G(\theta, a; t - t_a)G(\zeta, b; t - t_b)G(d, \delta; t_d - t) \\
& \times \langle ab | \Gamma(t_a, t_b, t_c, t_d) | cd \rangle G(c, \beta; t_c - t'), \quad (10.23)
\end{aligned}$$

where the symmetry of V and Γ was used under exchange. By returning to the energy formulation it is possible to show that Eq. (10.23) represents the Dyson equation. To perform this transformation it is useful to consider all the terms in Eq. (10.23) separately. First one notes that the time derivative of G can be written as

$$\begin{aligned}
i\hbar \frac{\partial}{\partial t} G(\alpha, \beta; t - t') = & i\hbar \frac{\partial}{\partial(t - t')} \int \frac{dE}{2\pi\hbar} e^{-\frac{i}{\hbar}E(t-t')} G(\alpha, \beta; E) \\
= & \int \frac{dE}{2\pi\hbar} e^{-\frac{i}{\hbar}E(t-t')} \{E G(\alpha, \beta; E)\}, \quad (10.24)
\end{aligned}$$

using Eq. (9.59). The term with the δ -function yields in a similar way

$$\delta(t-t')\delta_{\alpha,\beta} = \int \frac{dE}{2\pi\hbar} e^{-\frac{i}{\hbar}E(t-t')} \{\delta_{\alpha,\beta}\}. \quad (10.25)$$

Continuing with the next two terms one has

$$\varepsilon_\alpha G(\alpha, \beta; t-t') = \int \frac{dE}{2\pi\hbar} e^{-\frac{i}{\hbar}E(t-t')} \{\varepsilon_\alpha G(\alpha, \beta; E)\} \quad (10.26)$$

and

$$\begin{aligned} & - \sum_{\delta} \langle \alpha | U | \delta \rangle G(\delta, \beta; t-t') = \\ & \int \frac{dE}{2\pi\hbar} e^{-\frac{i}{\hbar}E(t-t')} \left\{ - \sum_{\delta} \langle \alpha | U | \delta \rangle G(\delta, \beta; E) \right\}. \end{aligned} \quad (10.27)$$

The first term containing the two-body interaction can be written as

$$\begin{aligned} & -i\hbar \sum_{\delta\zeta\theta} \langle \alpha\delta | V | \theta\zeta \rangle G(\zeta, \delta; t-t^+) G(\theta, \beta; t-t') = \\ & \int \frac{dE}{2\pi\hbar} e^{-\frac{i}{\hbar}E(t-t')} \left\{ -i \sum_{\delta\zeta\theta} \langle \alpha\delta | V | \theta\zeta \rangle \int_{C^+} \frac{dE'}{2\pi} G(\zeta, \delta; E') G(\theta, \beta; E) \right\}, \end{aligned} \quad (10.28)$$

where Eq. (9.60) has been used for the sp propagator with the equal time arguments. The last term in Eq. (10.23) can finally be written as

$$\begin{aligned} & -\frac{1}{2}(i\hbar)^2 \sum_{\delta\zeta\theta} \sum_{abcd} \int dt_a \int dt_b \int dt_c \int dt_d \{ \langle \alpha\delta | V | \theta\zeta \rangle \\ & \quad \times G(\theta, a; t-t_a) G(\zeta, b; t-t_b) G(d, \delta; t_d-t) \\ & \quad \times \langle ab | \Gamma(t_a, t_b, t_c, t_d) | cd \rangle G(c, \beta; t_c-t') \\ & = \int \frac{dE}{2\pi\hbar} e^{-\frac{i}{\hbar}E(t-t')} \left\{ \frac{1}{2} \sum_{\delta\zeta\theta} \sum_{abcd} \langle \alpha\delta | V | \theta\zeta \rangle \right. \\ & \quad \times \int \frac{dE_1}{2\pi} \int \frac{dE_2}{2\pi} G(\theta, a; E_1) G(\zeta, b; E_2) G(d, \delta; E_1 + E_2 - E) \\ & \quad \left. \times \langle ab | \Gamma(E_1, E_2, E, E_1 + E_2 - E) | cd \rangle G(c, \beta; E) \right\}. \end{aligned} \quad (10.29)$$

The combined results of Eqs. (10.24) - (10.29) demonstrate that Eq. (10.23) can be written as the inverse FT of an expression where several factors multiply $G(\alpha, \beta; E)$. Adding these factors and dividing this expression by

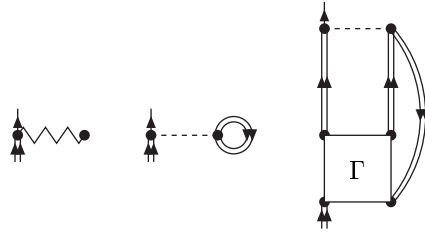


Fig. 10.13 Diagrams representing the irreducible self-energy as given by Eq. (10.31).

this sum one arrives at the following result for the inverse FT after some minor relabeling of dummy indices

$$G(\alpha, \beta; E) = G^{(0)}(\alpha, \beta; E) + \sum_{\gamma, \delta} G^{(0)}(\alpha, \gamma; E) \Sigma^*(\gamma, \delta; E) G(\delta, \beta; E), \quad (10.30)$$

which obviously is identical with the Dyson Equation when one identifies the irreducible self-energy with

$$\begin{aligned} \Sigma^*(\gamma, \delta; \omega) = & -\langle \gamma | U | \delta \rangle - i \int_{C \uparrow} \frac{dE'}{2\pi} \sum_{\mu, \nu} \langle \gamma \mu | V | \delta \nu \rangle G(\nu, \mu; E') \\ & + \frac{1}{2} \int \frac{dE_1}{2\pi} \int \frac{dE_2}{2\pi} \sum_{\epsilon, \mu, \nu, \zeta, \rho, \sigma} \langle \gamma \mu | V | \epsilon \nu \rangle G(\epsilon, \zeta; E_1) G(\nu, \rho; E_2) \\ & \times G(\sigma, \mu; E_1 + E_2 - E) \langle \zeta \rho | \Gamma(E_1, E_2; E, E_1 + E_2 - E) | \delta \sigma \rangle. \end{aligned} \quad (10.31)$$

This result is diagrammatically shown in Fig. 10.13. In this figure the

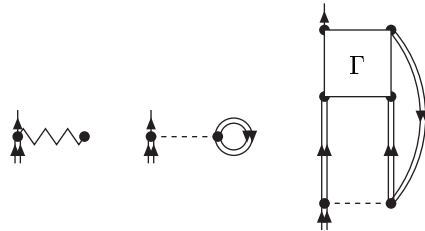


Fig. 10.14 Diagrams representing the irreducible self-energy as obtained by considering the equation of motion of G as a function of t' .

incoming line at the bottom of each self-energy diagram is represented by a short double line to signify a dressed propagator whereas the outgoing line corresponds to a noninteracting propagator identified by a single line. These last two contributions to the irreducible self-energy can easily be identified as the product of the dressed but noninteracting propagators in G_{II} giving rise to the second term in Eq. (10.31) (middle diagram) and the contribution containing Γ yielding the last term (and last diagram). The first term refers to the auxiliary sp potential.

This result is extremely useful since together with the Dyson equation itself, it provides a nonlinear formulation of the many-particle problem. It also includes some very intuitive notions which relate to the idea of a particle with modified properties in the medium (Dyson equation) which result from the interaction of the particle with the other particles Eq. (10.31). This interaction in turn takes place between particles immersed in the medium and therefore involves dressed particles. This nonlinearity is visible in the Dyson equation (Eq. (10.2)) for the sp propagator, which contains the self-energy (Eq. (10.31)) which in turn depends on the sp propagator. Self-consistency is therefore essential and unavoidable in developing calculational schemes. It also appears plausible that for stronger correlations in the system this self-consistency concept or, equivalently, the degree of nonlinearity, will be more important. Using the structure of the theory as outlined above, it becomes possible to develop nonlinear approximation schemes which take the dominant physical characteristics of the system into account. By identifying suitable approximations to G_{II} one has through Eq. (10.31) an appropriate calculational scheme that takes the corresponding physics into account. In many cases the interaction between the particles V dictates a certain minimum approximation for such a scheme to have a change of realistically describing the many-body system under study. In other cases the size of the system and the form of the interaction combine to dictate such a “minimum” approximation scheme. In its simplest form the diagrammatic version of the Hartree-Fock method is obtained. This method will be discussed in the next chapter.

10.5 Schrödinger-like equation from the Dyson equation

It is useful to illustrate at this point that the Dyson equation can generate a Schrödinger-like equation as was promised in Ch. 8 when experimental data related to removal probabilities were discussed. Indeed, by following similar

steps as in Sec. 7.3 one can obtain this result. We will discuss here the case when the spectrum for the $A \pm 1$ near the Fermi energy involves discrete bound states which mostly applies to finite system like atoms and nuclei. An appropriate form of the Lehmann representation in such a system is similar to Eq. (7.23) (allowing for hole propagation) and is given by

$$\begin{aligned}
G(\alpha, \beta; E) = & \sum_m \frac{\langle \Psi_0^A | a_\alpha | \Psi_m^{A+1} \rangle \langle \Psi_m^{A+1} | a_\beta^\dagger | \Psi_0^A \rangle}{E - (E_m^{A+1} - E_0^A) + i\eta} \\
& + \int_{\varepsilon_T^+}^{\infty} d\tilde{E}_\mu^{A+1} \frac{\langle \Psi_0^A | a_\alpha | \Psi_\mu^{A+1} \rangle \langle \Psi_\mu^{A+1} | a_\beta^\dagger | \Psi_0^A \rangle}{E - \tilde{E}_\mu^{A+1} + i\eta} \\
& + \sum_n \frac{\langle \Psi_0^A | a_\beta^\dagger | \Psi_n^{A-1} \rangle \langle \Psi_n^{A-1} | a_\alpha | \Psi_0^A \rangle}{E - (E_0^A - E_n^{A-1}) - i\eta} \\
& + \int_{-\infty}^{\varepsilon_T^-} d\tilde{E}_\nu^{A-1} \frac{\langle \Psi_0^A | a_\beta^\dagger | \Psi_n^{A-1} \rangle \langle \Psi_n^{A-1} | a_\alpha | \Psi_0^A \rangle}{E - \tilde{E}_\nu^{A-1} - i\eta}, \quad (10.32)
\end{aligned}$$

where the continuum energy spectrum for the $A \pm 1$ systems has been included and the corresponding energy thresholds are denoted by ε_T^\pm . A change of integration variable was also used to obtain this form of the Lehmann representation. For the unperturbed propagator one will encounter sp energies associated with H_0 that are different from those of G for any approximation made to the self-energy. This feature can be used to proceed taking limits of the Dyson equation in complete analogy with the limits taken in Sec. 7.3. The only difference that must be considered is associated with the energy dependence of the self-energy. This energy dependence of the self-energy will have certain properties depending on the chosen approximation. By exploring the equations of motion of the two-body propagator, it is possible to show that a Lehmann representation exists for the exact self-energy that has different poles from the one for G . In the subsequent chapters we will introduce approximation schemes to the self-energy that conform to this property. As a result, one may proceed with taking the following limit of the Dyson equation for the case of the hole part of the propagator without generating contributions from the poles in the self-energy or the noninteracting propagator

$$\begin{aligned}
\lim_{E \rightarrow \varepsilon_n^-} (E - \varepsilon_n^-) \left\{ G(\alpha, \beta; E) = \right. \\
\left. G^{(0)}(\alpha, \beta; E) + \sum_{\gamma\delta} G^{(0)}(\alpha, \gamma; E) \Sigma^*(\gamma, \delta; E) G(\delta, \beta; E) \right\}, \quad (10.33)
\end{aligned}$$

where the short-hand notation

$$\varepsilon_n^- = E_0^A - E_n^{A-1} \quad (10.34)$$

has been introduced. As for the *sp* problem this limit process generates an eigenvalue equation of the following kind (in complete analogy with the development in Ch. 7)

$$z_\alpha^{n-} = \sum_{\gamma, \delta} G^{(0)}(\alpha, \gamma; \varepsilon_n^-) \Sigma^*(\gamma, \delta; \varepsilon_n^-) z_\delta^{n-}, \quad (10.35)$$

where

$$z_\alpha^{n-} = \langle \Psi_n^{A-1} | a_\alpha | \Psi_0^A \rangle. \quad (10.36)$$

Since the Dyson equation can be written in a *sp* basis different from the one associated with H_0 , one may choose the coordinate representation with *sp* quantum numbers \mathbf{r}, m for the position and spin projection, respectively, to solve Eq.(10.35), one obtains

$$z_{\mathbf{r}m}^{n-} = \sum_{m_1, m_2} \int d^3 r_1 \int d^3 r_2 G^{(0)}(\mathbf{r}m, \mathbf{r}_1 m_1; \varepsilon_n^-) \Sigma^*(\mathbf{r}_1 m_1, \mathbf{r}_2 m_2; \varepsilon_n^-) z_{\mathbf{r}_2 m_2}^{n-}. \quad (10.37)$$

The unperturbed propagator, $G^{(0)}$, and the self-energy, Σ^* , require a *sp* basis transformation on both indices in order to obtain this result when originally the basis associated with H_0 was employed. Equation (10.37) can be rearranged by inverting the unperturbed propagator according to

$$\sum_m \int d^3 r \langle \mathbf{r}' m' | \varepsilon_n^- - H_0 | \mathbf{r} m \rangle G^{(0)}(\mathbf{r}m, \mathbf{r}_1 m_1; \varepsilon_n^-) = \delta_{m', m_1} \delta(\mathbf{r}' - \mathbf{r}_1), \quad (10.38)$$

using Eq.(8.39). The corresponding operation on $z_{\mathbf{r}m}^{n-}$ yields

$$\sum_m \int d^3 r \langle \mathbf{r}' m' | \varepsilon_n^- - H_0 | \mathbf{r} m \rangle z_{\mathbf{r}m}^{n-} = \left\{ \varepsilon_n^- + \frac{\hbar^2 \nabla'^2}{2m} - U(\mathbf{r}') \right\} z_{\mathbf{r}' m'}^{n-}, \quad (10.39)$$

where U is assumed to be local and spin-independent for simplicity. Combining these results yields the explicit cancellation of the auxiliary potential U and the following result

$$-\frac{\hbar^2 \nabla^2}{2m} z_{\mathbf{r}m}^{n-} + \sum_{m_1} \int d^3 r_1 \Sigma^*(\mathbf{r}m, \mathbf{r}_1 m_1; \varepsilon_n^-) z_{\mathbf{r}_1 m_1}^{n-} = \varepsilon_n^- z_{\mathbf{r}m}^{n-}. \quad (10.40)$$

This equation has the form of a Schrödinger equation with a nonlocal potential which is represented by the self-energy. Note that an eigenvalue ε_n^- can only be obtained when it coincides with the energy argument of the self-energy. An important difference with the ordinary Schrödinger equation is related to the normalization of the quasihole “eigenfunctions” $z_{\mathbf{r}m}^{n-}$. The appropriate normalization condition is obtained by performing the same steps that lead to Eq.(7.37). This result is most conveniently expressed in terms of the sp state which corresponds to the quasihole wave function $z_{\mathbf{r}m}^n$. In other words, one can use the eigenstate which diagonalizes Eq. (10.40), to express the normalization condition. Assigning the notation α_{qh} to this sp state, one obtains

$$|z_{\alpha_{qh}}^{n-}|^2 = \left(1 - \frac{\partial \Sigma(\alpha_{qh}, \alpha_{qh}; E)}{\partial E} \Big|_{\varepsilon_n^-}\right)^{-1}. \quad (10.41)$$

The subscript qh refers to the quasihole nature of this state and the fact that for states very near to the Fermi energy with quantum numbers corresponding to fully occupied mean-field states the normalization yields a number of order 1.

10.6 Exercises

- (1) Determine the expressions for the self-energy contributions in Fig. 10.6 using the energy formulation.
- (2) Generate all self-energy diagrams for the self-energy in the unsymmetrized version and determine the corresponding expressions.
- (3) Perform the steps that lead to the diagrammatic version of the irreducible self-energy shown in Fig. 10.14. Start by considering the derivative of $G(\alpha, \beta; t - t')$ with respect to t' .
- (4) Determine the form of the irreducible self-energy in the time formulation by using Eq. (10.23).
- (5) Derive Eq. (10.41).